

Restructuring Butterfat Through Blending and Chemical Interesterification. 2. Microstructure and Polymorphism

Dérick Rousseau, Arthur R. Hill, and Alejandro G. Marangoni*

Department of Food Science, University of Guelph, Guelph, Ontario N1G 2W1, Canada

ABSTRACT: Blending of butterfat with canola oil and subsequent chemical interesterification modified the crystal morphology and X-ray diffraction patterns of butterfat, 90:10 (w/w), and 80:20 (w/w) blends of butterfat–canola oil. The morphology of 50:50 (w/w) was also greatly influenced by interesterification.

Polarized light microscopy revealed that addition of canola oil led to gradual aggregation of the crystal structure. Scanning electron microscopy revealed all samples to be mixtures of defined crystalline regions and amorphous areas with greater amorphism as oil content increased. Most samples revealed segregation of solid from liquid. Confocal laser scanning microscopy of butterfat revealed complex aggregated structures that were composed of outwardly radiating filaments from a central nucleus. X-ray diffraction analysis revealed a predominance of β' and a small proportion of β crystals for all samples examined except interesterified butterfat, which consisted solely of β' crystals.

*JAOC*S 73, 973–981 (1996).

KEY WORDS: Confocal laser scanning microscopy, polarized light microscopy, scanning electron microscopy, X-ray diffraction.

Germane to a thorough understanding of plastic fat rheology is a characterization of its microstructure. Plastic fats consist of a crystal network in a continuous oil matrix. Fat crystals, which consist of interacting triacylglycerol (TAG) molecules in an asymmetrical tuning fork geometry (1), exhibit polymorphism. TAG with identical fatty acids can show large differences in polymorphic behavior (2). The current crystal polymorph nomenclature, proposed by Lutton (3), consists of three main forms— α , β' , and β . The α -form chain packing is hexagonal, the β' -form orthorhombic, while the β -form is triclinic (4). Crystal subforms include sub- α , $\beta'1$, $\beta'2$, pseudo- β' , sub- β , $\beta1$, and $\beta2$ (5).

Many factors influence lipid crystallization, notably how the sample is cooled from the melt (rate, initial, and final temperatures), duration of crystallization (e.g., aging), TAG organization, and fatty acid composition (6,7). Larsson (8) stated that two factors are involved in the formation of a three-dimensional crystal structure: effective packing into unit layers and stacking of these unit layers.

X-ray diffraction, used to identify crystal polymorphs, is based on the determination of the long and short spacings of crystals. The α -form has a single short spacing near 4.15 Å, the β' -form has spacings at 3.8 and 4.2 Å or three at 4.27, 3.97, and 3.71 Å, but the β -form does not correspond to either of these forms and shows a single strong spacing at 4.6 Å (7,9).

Most fats exhibit polymorphism monotropically (10). When a transition occurs (e.g., from β' to β), the molecular chain packing of the TAG becomes less motile, resulting in a higher melting point.

Two distinct phenomena can be distinguished during fat crystallization—nucleation and growth (11). In the liquid state, order can persist at temperatures as much as 40°C above the melting point of a fat (12). As the temperature is lowered from the melt, embryonic crystals composed of high-melting TAG form the initial nuclei (13,14). They must be large enough to avert dissolution in the liquid portion of the lipid. As the temperature is decreased, fat crystal solubility in oil diminishes. Once the initial nuclei have avoided dissolution, they can catalyze subsequent nucleation.

Compound crystals contain two or more different molecular species and easily occur in the α form, given the loose molecular packing. They are not stable and tend to rearrange into pure crystals (13). The TAG of a mixed crystal will have the same polymorphic form and will behave as a pure component (15). Butterfat exhibits extensive mixed crystallization.

Many microscopy techniques are used in the study of fat crystallization. Polarized light microscopy (PLM) can distinguish between solid and liquid phases because crystals are anisotropic whereas liquid fat is isotropic (16). Scanning electron microscopy (SEM) permits the study of surface topography. Finally, confocal laser scanning microscopy (CLSM) is a recent microscopic technique that complements both conventional light microscopy and electron microscopy, and has been used in the study of food emulsions (17,18). CLSM has improved lateral (x-y) and axial (x-z) resolution over conventional light microscopy without disruption of structure (17,19).

Many studies on fat morphology found in the literature have dealt with butterfat or lard. Hoerr and Waugh (20) examined the microscopic, polymorphic, and baking characteristics of randomized (chemically interesterified) lard. With PLM,

*To whom correspondence should be addressed.

they found that rearranged lard consisted of small spherulites rather than large spherulites in the native lard. Spherulites may be defined as globular collections of clustered crystals (21). Wiedermann *et al.* (22) found that interesterification destroyed the spherulitic nature of native lard crystal structures. deMan (23) observed, by using PLM, that the crystal habit of interesterified milkfat was markedly changed from that of native milkfat. deMan (24) also examined the effects of cooling procedures on consistency, crystal structure, and solid fat content of milkfat. More recently, Fairley *et al.* (25) examined the effect of time on the crystal morphology of mixtures of tripalmitin and butterfat by PLM. They reported that morphology did not change greatly in time.

The chemical and physical properties of a fat are linked by its microstructure. There is no conclusive single theory that relates all properties of fats. However, cognizance of microstructure is an essential piece of the fat spread structure–function puzzle. The objective of the present study is to assess the morphological modifications of butterfat after blending with canola oil and chemical interesterification by means of PLM, SEM, and CLSM.

MATERIAL AND METHODS

Blend preparation and interesterification. Blend preparation and chemical interesterification were performed as described by Rousseau *et al.* (26). Noninteresterified is abbreviated to NIE, and interesterified to IE.

Butterfat crystal extraction. Butterfat crystals were extracted with isobutanol (Fisher, St. Louis, MO). To remove liquid without solubilizing the solid fat crystals, suspensions of fat (2–3 g) in isobutanol (1:40) were prepared at 4°C, and the fat was dispersed with a Tissu-Mizer at low speed. The mixture was allowed to stand for 24 h at 4°C, after which two distinct layers appeared. The top layer consisted of liquid oil and isobutanol while the lower layer consisted of liquid oil, isobutanol, and solid crystals. The top layer was removed with a Pasteur pipette, and the lower layer was resuspended in isobutanol. This procedure was repeated twice. The final crystal suspension was centrifuged (5000 rpm for 10 min at 5°C). After removal of the supernatant, the solid crystals were resuspended in isobutanol.

PLM. To prepare the samples for PLM studies, prechilled viewing slides (Fisher) were prepared by placing a small amount of the fat on the slide and adding a drop of paraffin oil (Fisher) to aid in dispersing the sample. A cover slip (Fisher) was then firmly pressed on top of the slide to remove excess liquid and air pockets. Visual magnification was 400×, while photographic magnification was 105×. An Olympus BH polarized light microscope (Tokyo, Japan), mounted with a PM-6 35-mm camera, was used. Photomicrographs were taken on Kodak T-Max 400 ISO film with 30–40-s exposure times. All manipulations were performed at 4°C. Many samples were examined, and each photomicrograph represents a typical field.

SEM. Small amounts of fat blend were placed on pre-

cooled (4°C) brass blocks, containing prechilled Tissue-Tek mounting medium, before being transferred to a cryo-preparation unit. Isobutanol-extracted fat crystals were placed on precooled (4°C) brass blocks, covered with a Whatman filter held in place by prechilled Tissue-Tek. The blocks were plunged into liquid nitrogen slush (–207°C). To obtain a view of internal sample surfaces, freeze-fracturing was performed on the frozen sample. No freeze-fracturing was required for the extracted fat crystals. Sublimation was performed at –80°C for 30 min to remove any ice crystals that could cover microstructure. After sublimation, the samples were sputter-coated with 30 nm of gold. Cryo-fixation was used instead of osmium tetroxide fixation because it allows visualization of more defined structure (16). Samples were viewed in a Hitachi (Tokyo, Japan) S-570 SEM maintained at –150 to –170°C. Accelerating voltages of 5 to 15 kV were used with magnifications ranging from 500 to 10,000×. An aperture of 50 mm was used with a condenser lens current setting of 5. Photographs were taken on Ilford FP4-Plus film. The images shown were typical for all samples examined.

CLSM. To prepare the samples for CLSM studies, precooled (4°C) viewing slides (Fisher) were prepared by placing a small amount of the butterfat on the slide. A drop of Nile Blue stain was then placed on the sample and mixed with a precooled spatula. A cover slip (Fisher) was then firmly pressed on top of the slide to remove excess liquid and air pockets.

Nile Blue stain was used to negatively stain butterfat crystals. This stain contains a protonated oxazine base, oxazone, and a free oxazine base. This lipophilic stain diffuses into the oil phase of a sample and generates a deep yellow fluorescence (18). Solid fat does not fluoresce.

The Bio-Rad MRC-600 (Mississauga, Ontario, Canada) series laser scanning confocal microscope with a krypton/argon mixed gas laser was coupled with a Nikon Optiphot microscope (Tokyo, Japan). A Nikon plan-apo 60/1.4 oil immersion lens with a 10× eyepiece was used for a visual magnification of 600×. The immersion oil was nonfluorescing. The laser intensity was 3%, and the confocal aperture was at setting 3. Both the gain setting and black level were at settings 5 or 6. The images were recorded, processed, and analyzed by using the software provided with the MRC-600 CLSM.

X-ray diffraction (XRD) spectroscopy. The polymorphic modifications of the NIE and IE butterfat and 90:10 and 80:20 butterfat–canola oil blend fat crystals were determined by powder XRD with a 601 Diffractis X-ray generator and a Guinier XRD camera, model FR 552 (Enraf-Nonius, Delft, Holland). The instrument was fitted with a copper X-ray tube. The sample holder was a 1-mm flat stainless-steel plate with a rectangular opening in the middle. Samples were held in place with clear adhesive tape. The film used was Kodak P100, and measurements were performed at 5°C (maintained by a circulating waterbath). An Enraf-Nonius Guinier viewer was used to estimate the distance between diffraction lines on

the film to evaluate the short spacings. Samples were solidified for 24 h at 5°C.

RESULTS AND DISCUSSION

PLM. Both blending of canola oil and chemical interesterification substantially altered the crystal morphology of butterfat. Figure 1A shows the noninteresterified butterfat (NIEBF) crystal network after 1 d of crystallization. A dense network of spherulites and ill-defined needles with no discernible regular pattern was visible. Most structural elements measured

10–25 μm in size. Figure 1B reveals that the interesterified butterfat (IEBF) crystal network was composed of spherulites of varying density, measuring $\sim 15 \mu\text{m}$, with a lacy network of small crystals. These results agree with the results of deMan (23), who found that milkfat interesterification caused a decrease in crystal size. The spherulites were structurally weak; slight agitation led to their dismemberment (27). Addition of 10% canola oil to butterfat (NIE90:10) resulted in a dilution of the butterfat structure with no substantial change in morphology (Fig. 1C). Fewer large crystals were visible, with only a few irregularly shaped aggregates present. Small

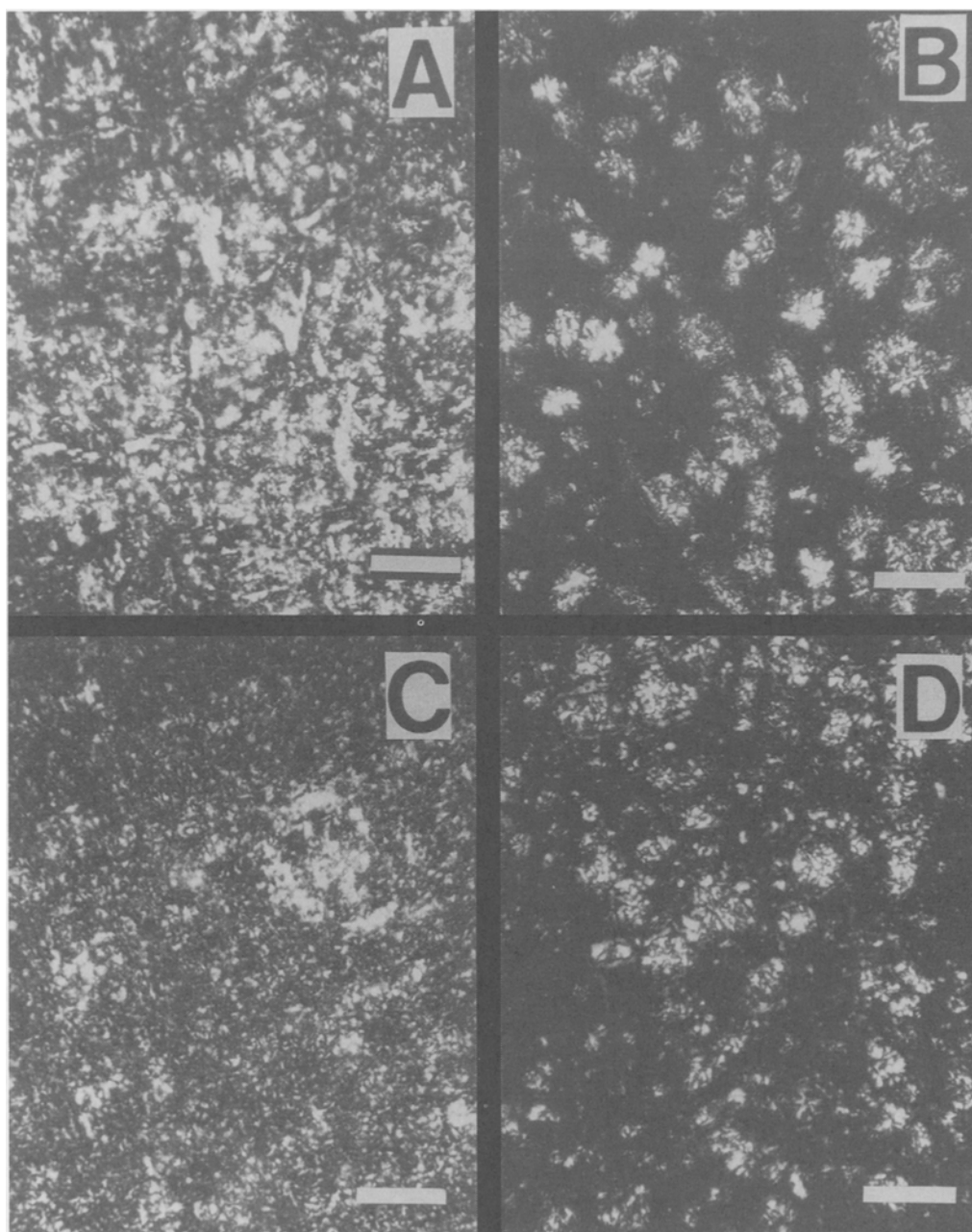


FIG. 1. Polarized light microscopy photomicrographs of samples tempered 24 h at 5°C. A, noninteresterified butterfat; B, interesterified butterfat; C, noninteresterified 90:10; and D, interesterified 90:10. The bar represents 25 μm .

needles, measuring only a few microns in size, comprised most of the crystals. Chemical interesterification of the 90:10 blend (IE90:10) (Fig. 1D) resulted in a morphology similar to that of IEBF.

Addition of 20% canola oil generated substantial morphological changes for the NIE80:20 blend, and the crystal network consisted of large and dense spherulites $\sim 20\ \mu\text{m}$ in size. Interesterification of the 80:20 blend (IE80:20) led to larger, more loosely packed spherulites, which measured $\sim 30\text{--}40\ \mu\text{m}$ in size. Small, disordered platelets were also discernible (Fig. 2B, inset), a commonality of chemically IE fats (28).

The NIE50:50 blend (Fig. 2C) was composed of small spherulites only $5\text{--}10\ \mu\text{m}$ in diameter. The interesterified sample (IE50:50) contained fewer crystals. At the magnification used, these crystals lacked structure and measured only a few microns in size.

The presence of canola oil substantially influenced the crystal morphology of butterfat. Because canola oil does not crystallize at temperatures above approximately -10°C (29), it will not be directly involved in any kind of crystallization with the butterfat. Other mechanisms must have come into play. Given that canola oil is $\sim 90\%$ C_{18} , it may have a slightly

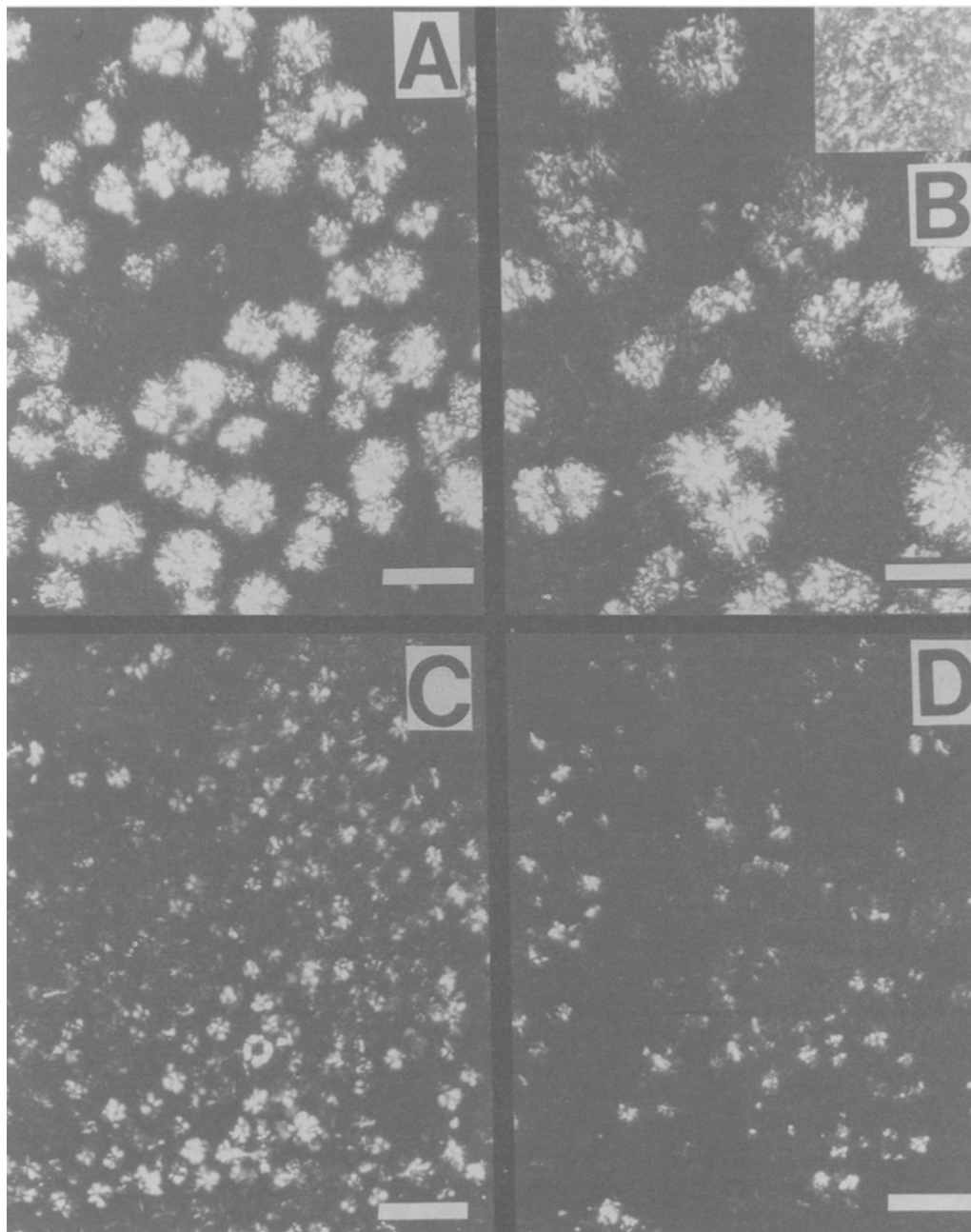


FIG. 2. Polarized light microscopy photomicrographs of samples tempered 24 h at 5°C . A, noninteresterified 80:20; B, interesterified 80:20; C, noninteresterified 50:50; and D, interesterified 50:50. The bar represents $25\ \mu\text{m}$.

higher hydrophobicity than butterfat. The difference in average chainlength between the butterfat and canola oil can possibly explain the patterns observed. During crystallization, canola oil TAG would not be easily interspersed among crystallizing butterfat molecules. Therefore, the formation of spherulites would be more likely.

In a perfect crystal, the surface free energy is close to zero. An increase in imperfection results in an increase in free energy. Larger crystals have lower surface energy compared with smaller crystals (20). Crystal aggregates have even lower surface energy (30). This phenomenon, known as

Ostwald ripening, is evident in Figures 1 and 2. The migration of crystals to form aggregates was most likely facilitated by the addition of canola oil because less solid fat is present to impede migration toward other crystals.

The presence of small crystals between large spherulites may be evidence for sintering, the formation of solid bridges in narrow gaps of fat crystal networks (31). Sintering is a form of strong adhesion created by the crystallization of a fat phase with a melting point between that of the oil phase and the crystal.

SEM and CLSM. Figure 3 shows the structure of NIEBF

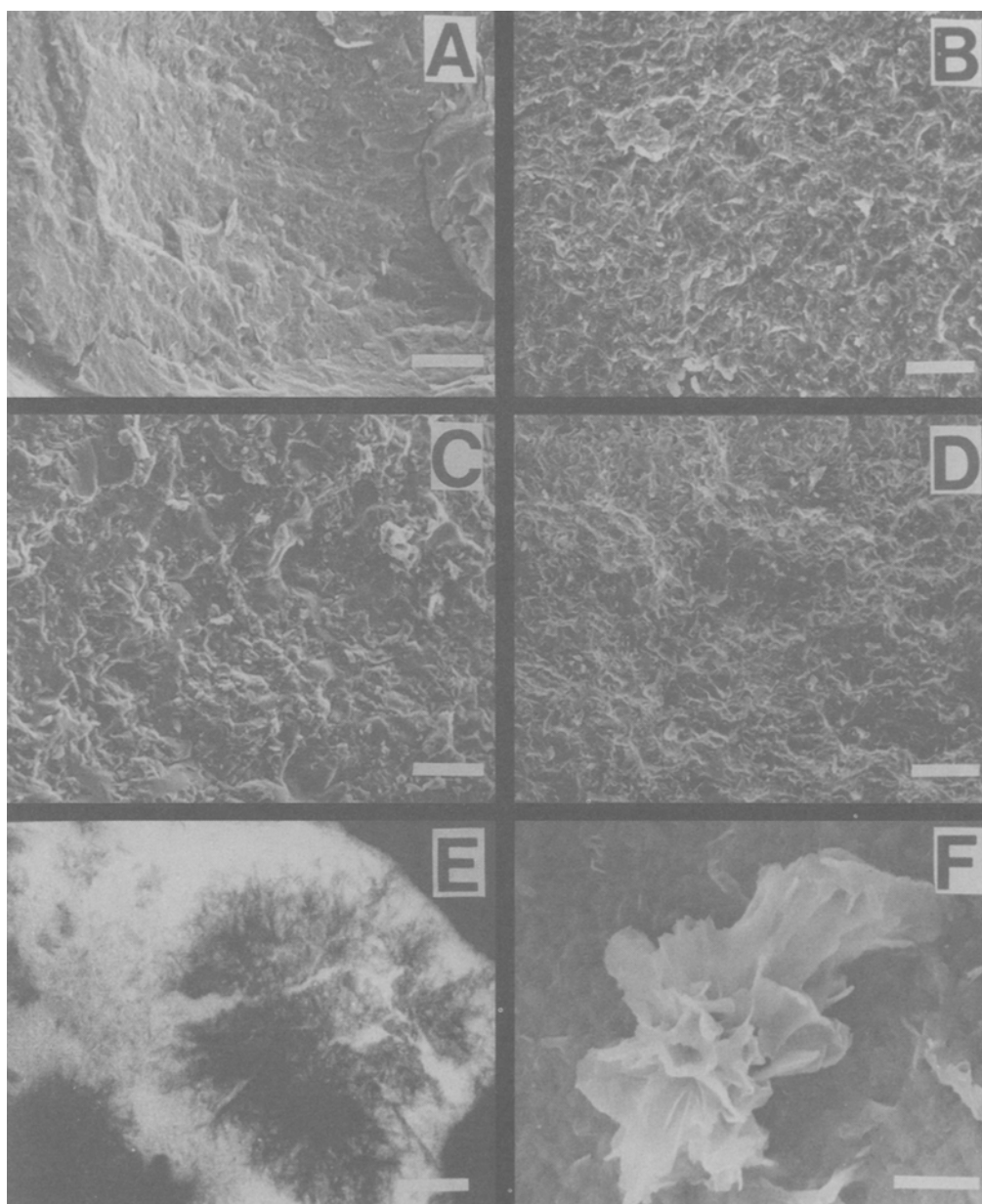


FIG. 3. Photomicrographs of butterfat tempered for 1 or 8 d at 5°C. A, Scanning electron microscopy (SEM), noninteresterified butterfat (NIEBF), 1 d; B, SEM, NIEBF, 8 d; C, SEM, interesterified butterfat (IEBF), 1 d; D, SEM, IEBF, 8 d; E, confocal laser scanning microscopy, NIEBF, 8 d; and F, SEM, isobutanol-extracted NIEBF, 8 d. The bar represents 25 μm for 3A–3E and 5 μm for 3F.

and IEBF tempered for 1 or 8 d at 5°C. Figure 3 (A–D and F) were produced by SEM and Figure 3E by CLSM.

The surface structure of butterfat after 1 d of crystallization (Fig. 3A) was poorly defined. High magnification (photomicrograph not shown) showed that the visible ridges were structured but not well ordered. Tempering for 8 d (Fig. 3B) revealed extensive mottling, indicative of crystal growth.

IEBF after 1 and 8 d of crystallization (Fig. 3, C and D, respectively) was comparatively more structured than NIEBF. After 8 d of crystallization, the surface of IEBF (Fig. 3D) was more finely detailed than the surface of NIEBF. This may

be due to greater recrystallization in the NIEBF compared with IEBF.

Figure 3E reveals a cross-sectional view of a butterfat aggregate by CLSM. The image suggests a well-resolved dendritic structure of the butterfat with a visible microstructure in the submicron range. The large aggregate measured $90\ \mu\text{m} \times 70\ \mu\text{m}$ and consisted of 3–4 different component aggregates within the main structure. From all groups, wispy filaments emanated from a central nucleus with extensive branching. It is quite possible that this branching was responsible for the formation of crystal bridges between different aggregates.

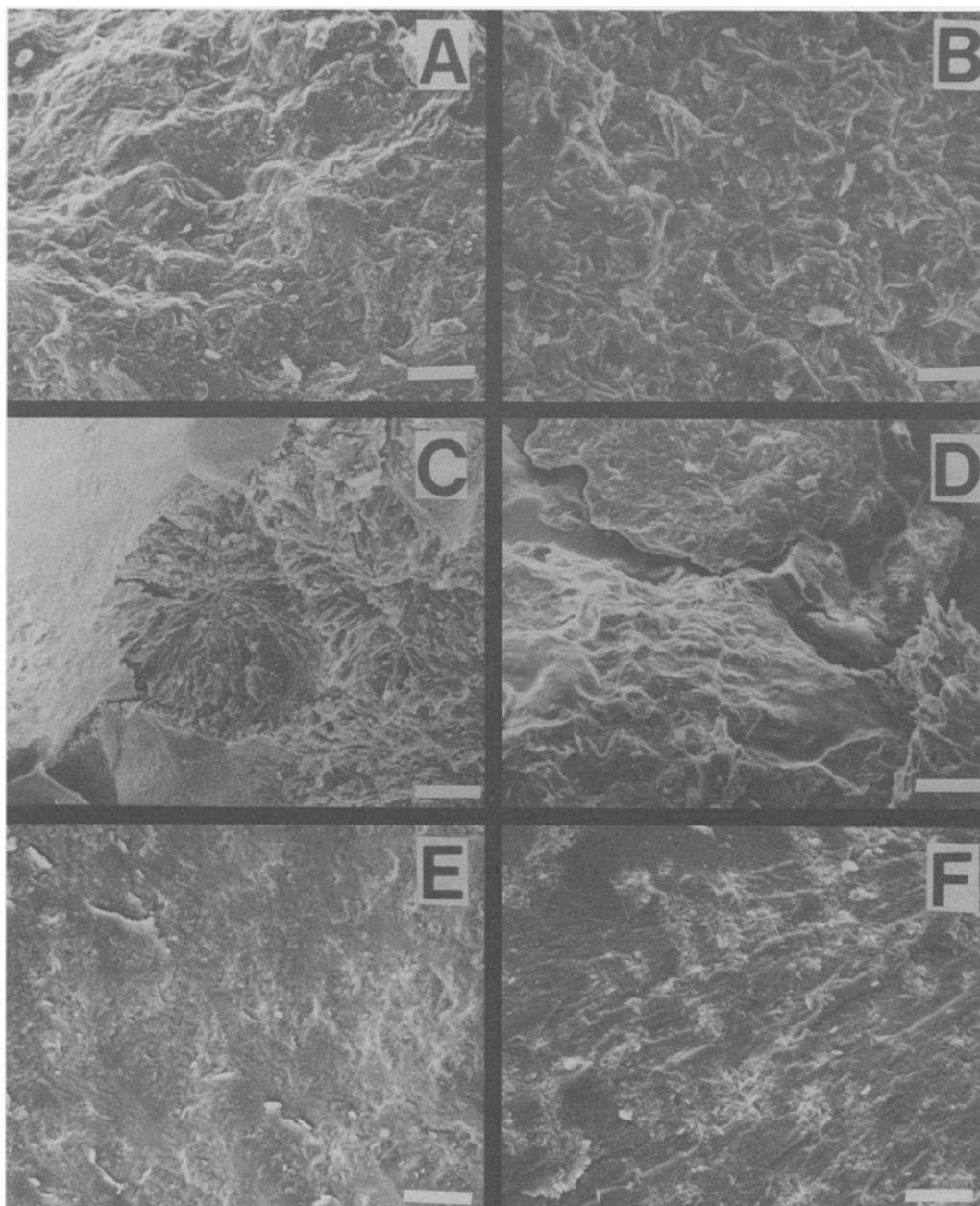


FIG. 4. SEM photomicrographs of blends tempered for 1 or 8 d at 5°C. A, IE90:10, 1 d; B, IE, 90:10, 8 d; C, NIE, 80:20, 8 d; D, IE, 80:20, 8 d; E, NIE, 50:50, 1 d; and F, IE, 50:50, 1 d. The bar represents 25 μm . See Figure 3 for abbreviations.

The interacting aggregates may suggest how larger aggregates form. Clear areas between the aggregates, in which only liquid oil was visible, may have arisen due to steric hindrance or may have represented areas in the initial stages of sintering. Figure 3F shows an isobutanol-extracted butterfat crystal. As with the CLSM results, a central nucleus was visible with outwardly radiating arms. The structure appeared as an oblong spherulite. While the isobutanol-extracted crystal and the CLSM images are on different scales, definite similarities are evident because both structures have a dense, well-defined nucleus with tenuous crystalline matter surrounding the central region.

Figure 4 shows the surface structure of various samples examined by SEM. Figure 4 (A and B) show the NIE90:10 blend after 1 and 8 d of tempering, respectively. Structure increased from day 1 to day 8. Figure 4 (C and D) show NIE80:20 and IE80:20 after 8 d of tempering, respectively. Surface structure was different for both blends. In the noninteresterified blend, a definite segregation of liquid and solid was visible that was not visible in the interesterified equivalent. Figure 4 (E and F) show NIE50:50 and IE50:50, respectively, after 1 d of tempering. Both samples appeared equally detailed but contained different structure. The NIE50:50 blend showed a relatively smooth surface, whereas the IE50:50 blend (Fig. 4F) revealed segregation of spherulitic agglomerates.

Figure 5A shows a high magnification view of NIE90:10 after 8 d of crystallization, while Figure 5B shows a close-up of butterfat structure after 8 d of crystallization. The NIE90:10 blend presented an extensive, haphazardly arranged structure. In Figure 5B, there appears to be layering in the butterfat crystal structure. This phenomenon was explored in great detail by Precht and Buchheim (32) who examined the fine structure of butter by transmission electron microscopy (TEM). While there was a 100-fold difference in scale between the present work and the work of Precht and Buchheim (32), there is an evident layering pattern visible in both studies. This shows that the repeating layer order in the structure may be partly responsible for the structure of three-dimensional crystal networks and seems self-similar in nature.

The examples of the effect of tempering and composition shown here represent an accurate cross-section of all examined specimens. The spherulites observed in the PLM photomicrographs were also present in the SEM equivalents; however, they were embedded in the solid-liquid matrix. This effect is particularly evident for the IE50:50 blend (Fig. 2D vs. Fig. 4F) and the IE90:10 blend (Fig. 1D vs. Fig. 4A).

During the cryo-preparation with liquid nitrogen, the cooling was rapid enough to prevent the formation of noticeable crystals in the liquid oil. This minimized the formation of artifacts, created upon freezing, because the liquid oil is solidified in an amorphous fine structure, void of detail. Jewell and Meara (33) observed the same phenomenon with cryo-fixed samples of lard and shortening when viewed with TEM.

For all samples examined, tempering was meticulously controlled. Even with identical tempering, great variations in

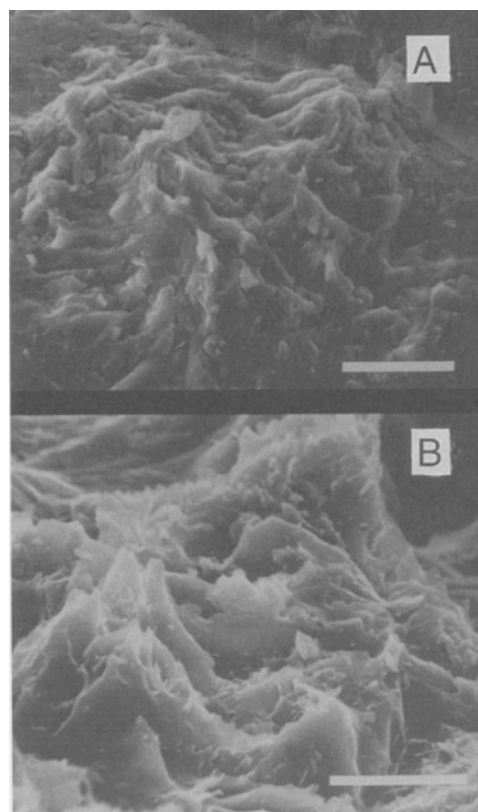


FIG. 5. Higher magnification scanning electron microscopy photomicrographs of blends tempered for 8 d at 5°C. A, NIEBF, 8 d; and B, NIE, 90:10, 8 d. The bar represents 10 µm. See Figures 3 and 4 for abbreviations.

morphology were apparent among all samples. Thus, the fatty acid and TAG composition were responsible for the variations in microstructure. Different proportions of canola oil, followed by randomization, resulted in different final morphologies. A more random TAG distribution resulted in a less organized structure as exemplified in both PLM and SEM results.

XRD spectroscopy. Table 1 details the polymorphic modifications engendered by blending and chemical interesterification. Other extremely weak bands appeared but were not considered in the final analysis. The XRD data reveal that most samples were combinations of β' and β crystals. Natural butterfat consisted primarily of β' crystals with a small proportion of β crystals, indicated by a weak spacing at ~ 4.6 Å. Interesterification of butterfat resulted in the removal of the band at 4.6 Å. Woodrow and deMan (34) and Timms (35) both reported XRD results for NIE and IE milkfat. Natural milkfat had strong short spacings at 3.8 and 4.2 Å, indicative of β' , plus a weak short spacing at 4.6 Å, indicative of the β polymorph. After interesterification with sodium-based catalysts, the short spacing at 4.6 Å had disappeared.

Replacement of 10% (w/w) butterfat with canola oil increased the relative intensity of the band at 4.6 Å, indicating a higher proportion of β content. Interesterification of the 90:10

TABLE 1
Polymorphic Forms and Short Spacings (Å) of Noninteresterified (NIE) and Interesterified (IE) Butterfat and 90:10 and 80:20 Blends with Canola Oil^a

| Blend | Short spacings (Å) | | | | Polymorph |
|-------|--------------------|-------|-------|-------|------------------|
| | 4.6 | 4.2 | 3.8 | 3.7 | |
| NIEBF | 4.62w | 4.19s | 3.80m | 3.75w | $\beta' > \beta$ |
| NIE90 | 4.57w | 4.19s | 3.80m | 3.71w | $\beta' > \beta$ |
| NIE80 | 4.60w | 4.23s | 3.83m | — | $\beta' > \beta$ |
| IEBF | — | 4.22s | 3.80m | — | β' |
| IE90 | 4.57vw | 4.21s | 3.81m | — | $\beta' > \beta$ |
| IE80 | 4.57w | 4.24s | 3.80m | — | $\beta' > \beta$ |

^aIntensities: v, very; w, weak; m, medium; s, strong.

blend generated β crystals with the appearance of a weak band at 4.6 Å only in small proportions. The reappearance of β crystals in the interesterified 90:10 blend is possibly due to lack of variety in chainlength. A means of stabilizing the β' modification is to have TAG with varying chainlengths. As stated by Larsson (30), variations in chainlength result in a more disordered packing near the methyl end regions, leading to less chance of a tightly knit crystal lattice. Because β crystals have the most ordered structure, a decrease in chainlength variety will increase their likelihood. For both NIEBF and NIE90:10, a weak band at ~ 3.73 Å was present, indicative of a possible crystal subform. Both 80:20 blends contained larger amounts of β crystals than the 90:10 blends. The increased canola oil content led to an increase in β content.

The crystal polymorph has primordial importance for final product consistency and acceptability. Smaller crystals lead to firmer fat products, whereas larger fats give a sense of sandiness in the mouth. Incorporation of large amounts of liquid oil increases the tendency of the desirable β' polymorphic form to convert to the β form (36). In the production of butterfat–canola oil spreads, preserving the β' form would be essential to avoid a sandy mouth feel.

Structure and polymorphic form. Van den Tempel (37) surmised that the structure of a fat crystal network consisted of an assembly of chains, each chain being an assembly of a linear array of closely aligned particles. The chains were considered to be branched and interlinked to form a three-dimensional network, with liquid fat filling the voids. Unfortunately, this theory did not successfully account for the nonlinear dependence of rheological phenomena, such as yield stress and elastic modulus, on the proportion of solid fat. Fat crystal networks are now viewed as composed of haphazardly interlinked aggregates (38). Network properties depend on the elastic nature of the individual aggregates (39,40).

Examination of Figures 1 and 2 reveals aggregated structure for many samples. This aggregation behavior represents reality in terms of network structure.

β -Crystals are considered the most stable crystal polymorph (3). In the examined samples, as the proportion of oil increased, so did the presence of β -crystals. Microstructurally, aggregation in the form of spherulites became more pro-

nounced. Aggregation behavior was also more apparent in the IE samples than in the NIE samples. IEBF was devoid of β -crystals, yet demonstrated substantial aggregation. Thus, aggregation in fat crystals cannot be readily explained by polymorphic form. Other factors, such as viscosity of the liquid phase, composition, and tempering must have come into play.

At a cursory level, this study has shown that microstructure is heavily influenced by blending and chemical interesterification, and that polymorphism and microstructure are not directly linked.

ACKNOWLEDGMENTS

The authors express their gratitude to Dr. J.M. deMan for use of his polarized light microscope and X-ray diffraction unit, and to L. deMan for helpful comments regarding polarized light microscopy. Funding from the Ontario Ministry of Agriculture, Food and Rural Affairs (Ontario Food Processing Research Fund) and the Natural Sciences and Engineering Research Council (NSERC) is greatly appreciated.

REFERENCES

- Jensen, L.H., and A.J. Mabis, Crystal Structure of β -Tricaprin, *Nature* 197:681–682 (1963).
- Rossell, J.B., in *Advances in Lipid Research*, edited by R. Padetti and D. Kritchevsky, Academic Press, New York, 1967, pp. 353–408.
- Lutton, E.S., Review of the Polymorphism of Saturated Even Glycerides, *J. Am. Oil Chem. Soc.* 27:276–281 (1950).
- Chapman, D., The Polymorphism of Glycerides, *Chem. Rev.* 62:433–456 (1962).
- D'Souza, V., J.M. deMan, and L.deMan, Short Spacings and Polymorphic Forms of Natural Fats and Commercial Solid Fats: A Review, *Ibid.* 67:835–843 (1990).
- Cebula, D.J., and K.W. Smith, Differential Scanning Calorimetry of Confectionary Fats. Pure Triglycerides: Effects of Cooling and Heating Rate Variation, *Ibid.* 68:591–595 (1991).
- deMan, J.M., X-Ray Diffraction in the Study of Fat Polymorphism, *Food Research International* 25:471–476 (1992).
- Larsson, K., Molecular Arrangements in Glycerides, *Fette Seifen Anstrichm.* 74:136–142 (1972).
- Larsson, K., Classification of Glyceride Crystal Forms, *Acta Chem. Scand.* 20:2255–2260 (1966).
- Manning, D.M., and P.S. Dimick, Crystal Morphology of Cocoa Butter, *Food Microstructure* 4:249–265 (1985).
- van Krevelen, D.W., and P.J. Hoftyzer, *Properties of Polymers: Correlations with Chemical Structures*, Elsevier Publishing Company, Amsterdam, 1972, pp. 301–310.
- Hernqvist, L., On the Structure of Triglycerides in the Liquid State and Fat Crystallization, *Fette Seifen Anstrichm.* 86:297–300(1984).
- Walstra, P., and R. Jenness, *The Chemistry and Physics of Milk Products and Comparable Foods*, The Universities Press, Belfast, 1974, pp. 88–97, 298–299.
- D'Souza, V., L. deMan, and J.M. deMan, Chemical and Physical Properties of the High Melting Glyceride Fractions of Commercial Margarines, *J. Am. Oil Chem. Soc.* 68:153–162 (1991).
- Bailey, A.E., *Melting and Solidification of Fats*, Interscience Publishers, New York, 1950, pp. 1–346.
- Chawla, P., J.M. deMan, and A.K. Smith, Crystal Morphology of Shortenings and Margarines, *Food Structure* 9:329–336 (1990).
- Heertje, P., P. Van der Vlist, J.C.G. Blonk, H.A.C.M. Hendriks, and G.J. Brakenhoff, Confocal Scanning Laser Microscopy in

- Food Research: Some Observations, *Food Microstructure* 6:115–120 (1987).
18. Heertje, P., J. Nederlof, H.A.C.M. Hendriks, and E.H. Lucassen-Reynders, The Observation of the Displacement of Emulsifiers by Confocal Scanning Laser Microscopy, *Food Structure* 9:305–316 (1990).
 19. Cheng, P.C., T.H. Lin, W.L. Wu, and J.L. Wu, *Multidimensional Microscopy*, Springer-Verlag, New York, 1994, pp. 1–289.
 20. Hoerr, G.W., and D.F. Waugh, Some Physical Characteristics of Rearranged Lard, *J. Am. Oil Chem. Soc.* 32:37–41 (1950).
 21. VanHook, A., *Crystallization: Theory and Practice*, Reinhold Publishing Corporation, New York, 1963, pp. 45–91.
 22. Wiedermann, L.H., T.J. Weiss, G.A. Jacobson, and K.F. Mattil, A Comparison of Sodium-Methoxide Treated Lards, *J. Am. Oil Chem. Soc.* 38:389–395 (1961).
 23. deMan, J.M., Physical Properties of Milk Fat. II. Some Factors Influencing Crystallization, *J. Dairy Res.* 28:117–123 (1961).
 24. deMan, J.M., Effect of Cooling Procedures on Consistency, Crystal Structure and Solid Fat Content of Milk Fat, *Dairy Ind.* 29:546–547 (1964).
 25. Fairley, P., J.M. Krochta, and J.B. German, Crystal Morphology of Mixtures of Tripalmitin and Butterfat, *J. Am. Oil Chem. Soc.* 72:693–697 (1995).
 26. Rousseau, D., K. Forestière, A.R. Hill, and A.G. Marangoni, Restructuring Butterfat Through Blending and Chemical Interesterification. I. Melting Behaviour and Triacylglycerol Modifications, *Ibid.* 73:963–972 (1996).
 27. deMan, J.M., and F.W. Wood, Polarized Light Microscopy of Butter-Fat Crystallization, *Proc. XV Int. Dairy Congr.* 2:1010–1016 (1959).
 28. Hoerr, C.W., Morphology of Fats, Oils, and Shortenings, *J. Am. Oil Chem. Soc.* 37:539–546 (1960).
 29. Riiner, Ü., Investigation of the Phase Behavior of *Cruciferae* Seed Oils by Temperature Programmed X-Ray Diffraction, *Ibid.* 47:129–133 (1970).
 30. Larsson, K., *Lipids—Molecular Organization, Physical Functions and Technical Applications*, The Oily Press, Dundee, 1994, pp. 1–41.
 31. Johansson, D., and B. Bergenståhl, Sintering of Fat Crystal Networks in Oil During Post-Crystallization Processes, *J. Am. Oil Chem. Soc.* 72:911–920 (1995).
 32. Precht, D., and W. Buchheim, Elektronenmikroskopische Untersuchungen über die physikalische Struktur von Streichfetten. II: Die Mikrostruktur des zwischenglobularen Fettphase in Butter, *Milchwissenschaft* 35:393–398 (1980).
 33. Jewell, G.G., and M.L. Meara, A New and Rapid Method for the Electron Microscopic Examination of Fats, *J. Am. Oil Chem. Soc.* 47:535–538 (1970).
 34. Woodrow, I.L., and J.M. deMan, Polymorphism in Milk Fat Shown by X-Ray Diffraction and Infrared Spectroscopy, *J. Dairy Sci.* 51:996–1000 (1961).
 35. Timms, R.E., The Physical Properties of Blends of Milk Fat with Beef Tallow and Beef Tallow Fractions, *Aust. J. Dairy Technol.* 34:60–65 (1979).
 36. deMan, L., J.M. deMan, and B. Blackman, Effect of Tempering on the Texture and Polymorphic Behaviour of Margarine Fats, *Fat Sci. Technol.* 97:55–60 (1995).
 37. van den Tempel, M., Mechanical Properties of Plastic Disperse Systems at Very Small Deformations, *J. Colloid Sci.* 16:284–296 (1961).
 38. van den Tempel, M., Rheology of Concentrated Suspensions, *J. Colloid Interface Sci.* 71:18–20 (1979).
 39. Kamphuis, H., and R.J.J. Jongschaap, The Rheological Behaviour of Suspensions of Fat Particles in Oil Interpreted in Terms of a Transient-Network Model, *Colloid and Polymer Sci.* 263:1008–1024 (1985).
 40. Kantor, Y., and I. Webman, Elastic Properties of Random Percolating Systems, *Phys. Rev. Lett.* 52:1891–1894 (1984).

[Received December 19, 1995; accepted April 18, 1996]